Analyst

ROYAL SOCIETY OF CHEMISTRY

PAPER

View Article Online
View Journal | View Issue

Cite this: *Analyst*, 2021, **146**, 3034

A homogeneous digital biosensor for circulating tumor DNA by the enumeration of a dual-color quantum dot complex

Xiaojun Liu,†[a] Zhangjian Wu,†[a] Xinyi Lin,[a] Wei Bu,*[b] Lei Qin[c] and Hongwei Gai *[a]

Received 17th February 2021,
Accepted 18th March 2021

DOI: 10.1039/d1an00299f

rsc.li/analyst

Monitoring ctDNA in blood is important for cancer management. Here, a one-step single particle counting approach was developed for directly quantifying ctDNA in plasma. Hairpin DNA containing a triple helix stem was immobilized onto QD 585 as a probe. The hairpin was opened by the target, and therefore hybridized with assistant DNA on QD 655, resulting in an aggregate of QD 585 and QD 655. The two-color QD aggregate was regarded as the target. Observed under a single particle transmission grating-based spectral microscope, the two-color QD aggregate was distinguished by a unique spectral pattern of two first-order streaks, and it was counted. The difference in the responses of the probes to perfect-match DNA, single-base mismatch DNA, and non-match DNA indicated that the probe had sufficient single-base discrimination capabilities. The success in plasma recovery tests demonstrated the feasibility of carrying out the direct detection of ctDNA in plasma.

Introduction

Circulating tumor DNA (ctDNA) that is released into blood by tumor cells carries genetic and epigenetic mutations of the tumor.[1,2] The half-time of ctDNA is below 2.5 hours, whereas that of the protein biomarker ranges from days to weeks.[3] Therefore, the ctDNA level is more suitable for reflecting tumor progress in real time. Monitoring ctDNA may revolutionize each step of cancer management, such as early detection, minimal residue assessment, treatment response, and tumor development.[3–5] For example, the ctDNA level indicates tumor recurrence long before clinical imaging, with an average lead time ranging from five months to 11.8 months.[3,5]

Rare ctDNA and rich wild-type DNA released by normal cells exist in blood together, which makes it a challenge to quantify ctDNA.[6–10] The vast majority of the approaches for quantifying ctDNA require target amplification by PCR, including real-time PCR, digital PCR, BEAMing, droplet digital PCR,[7] CAPP-Seq, Tam-Seq, and cSMART-Seq. Use of PCR adheres rigorously to complicated thermocycling: heat denaturation–renaturation–heat denaturation, which causes chemical damage to DNA polymerases. The chemical damage and imperfect copying of the DNA polymerases cause exponential amplification of non-target DNA, resulting in significant false positive results.[11–13] These PCR-based methods require the extraction of the DNA from the blood. The extraction introduces wide variation in quantity and integrity of ctDNA.[3,14] As an example, the concentrations of cell free DNA extracted from the same blood sample by 56 laboratories throughout Europe varied from 2.87 to 224.02 pg μL^{-1}.[14] Therefore, a method that is capable of directly quantifying ctDNA in blood without PCR amplification and DNA extraction is required urgently.

In 2015, a pioneering work on directly quantifying ctDNA in serum was reported by Kelley and co-workers.[15] In their study, the wild-type DNA and the non-target ctDNA were masked by a series of clamp molecules, and the hybridization of the target ctDNA with the capture probe immobilized on the surface of an electrode which triggered an electrochemical signal. Multi-branched, 3-D micro-electrodes were used to increase the amount of the capture probe, therefore greatly enhancing the hybridization efficiency between the target and the capture probe. The same strategy was adapted in follow-up research.[16] In 2019, an approach based on SERS was developed for directly determining ctDNA in serum.[17] Two techniques were used to enhance the signal. One was that the target was recycled through the RNase HII enzyme to specifically separate the complex of the recognition molecule and the target. Another was that a silver nanoparticle film was used to increase the loading amount of the SERS reporter. In 2020, a new enhancement strategy for the electrochemical signal was established.[18]

[a]*School of Chemistry and Materials Science, Jiangsu Normal University, Shanghai Road 101, Xuzhou, Jiangsu, China. E-mail: gai@jsnu.edu.cn*
[b]*Key Laboratory of Biotechnology for Medicinal Plant of Jiangsu Province, School of Life Science, Jiangsu Normal University, Xuzhou, Jiangsu, China. E-mail: buweijssf@163.com*
[c]*Xuzhou Haichuan Institute of Life Science Co. Ltd, Xuzhou, Jiangsu, China*
†These authors contributed equally.

The double strand complex of the target ctDNA and the recognition molecule was extended, which created more binding sites for the capture probe and thus greatly increased the sensitivity. In short, sophisticated signal enhancement is essential for the direct interrogation of ctDNA in blood. This required either complicated, time-consuming preparation of the sensor or restricting the control of the reaction conditions. The previously described sensing process required multi-cycles of separation and washing to remove the reactants unbound to the sensor. Each cycle increased determination time and cumulative errors.

Single particle detection can count the number of molecules without any chemical amplification or enrichment steps,[19,20] and may be an alternative way to directly quantify ctDNA in blood. Single particle detection can reveal particle heterogeneity that is not detectable in an ensemble detection system, which makes it possible to quantify the target without separation.[21,22] For example, using a fluorescent single particle spectral imaging microscope it was possible of judging whether quantum dots (QDs) of the same color were dispersed or aggregated by their spectral blue-shift pattern.[23,24] In these assays, the spectral blue-shift usually took more than 10 minutes. To address this, an approach for judging the dispersion state of two-color QDs was developed, and was used to directly quantify ctDNA in serum. The DNA hairpin with a triple helix stem was immobilized onto a QD 585 and the assembly was used as a recognition probe. The hairpin was opened by the target, and therefore hybridized with the assistant DNA (asDNA) immobilized onto a QD 655. Put simply, a target ctDNA induced a two-color QD aggregate (QD 585 and QD 655), and in turn, a two-color QD aggregate could be regarded as a target ctDNA. Under a single particle transmission grating-based spectral microscope, the two-color QD aggregate was distinguished by the unique spectral pattern of the two first-order streaks and counted. The responses of the probes to the perfect-match DNA, the single-base mismatch DNA, and the non-match DNA were quite different, indicating that the probes had a single-base discrimination capability. The success in a plasma recovery test indicated the feasibility of the direct detection of ctDNA in plasma. A single judgement on the two-color QD aggregate was finished within two minutes, which was an improvement when compared with that of the same-color QD aggregate.

Experimental section

Materials

Chemicals and materials. The DNA oligonucleotides of the KARS gene related to lung carcinoma were synthesized by the Shanghai Sangon Bioengineering Limited Company (Shanghai, China). The base sequences were: t1DNA: NH_2TTCCTCTCTCTCTGGAGCTGATGGCG TATCTCTCTCTC (5′ to 3′), t2DNA: AGAGAGAGAG (5′ to 3′), asDNA: NH_2TTCGAGAGAGA (5′ to 3′) (5′ to 3′), ctDNA: TACGCCATCAGCTCC (5′ to 3′), the single-base mismatched DNA: TACGCCACCAGCTCC (5′ to 3′), and the non-match DNA: CCTGTGCCGTGT (5′ to 3′). Carboxylic QD 655 (cat. no. Q21321MP), carboxylic QD 585 (cat. no. Q21311MP), blocking reagent (cat. no. 37580), and coverslips were obtained from ThermoFisher Scientific (Waltham, MA, USA). Glass slides were purchased from Citotest Labware Manufacturing Co., Ltd (Haimen, Jiangsu, China). Bovine serum albumin, chicken egg albumin, trypsin inhibitor, human serum albumin, phytohemagglutinin, transferrin, fibrinogen, poly(diallyldimethylammonium chloride), and *N*-(3-(dimethylamino)propyl)-*N*-ethylcarbodiimide hydrochloride (EDC) were purchased from Sigma-Aldrich (St Louis, MO, USA). A transmission grating with 70 lines per mm was obtained from Edmund Scientific (Barrington, NJ, USA).

Positively charged glass slide

The glass slide was immersed into chromic acid solution for 12 h and then ultrasonically washed three times with distilled water. Each wash lasted 15 min. The clean slide was placed into 1.0% (v/v) poly(diallyldimethylammonium chloride) (v/v) for 12 h, and then dried at 85 °C. The negatively charged QDs were able to deposit more easily and quickly on the positively charged slide than on the normal, negatively charged slide.

Probe preparation

The DNA hairpin with a triple helix stem and asDNA were immobilized onto QD 585 (TR-QD 585) and QD 655 (asDNA-QD 655), respectively. The TR-QD 585 was prepared in two steps: the t1DNA linking to carboxylic QD 585 (t1DNA-QD 585) and the immobilized t1DNA was hybridized with t2DNA. The t1DNA-QD 585 was prepared according to the manufacturer's procedure. A portion (20.0 μL) of 0.8 μM carboxylic QD 585 was activated with freshly prepared EDC, and then immediately mixed with 5.2 μL of 12.2 μM t1DNA. The mixture was shaken in darkness for 4.0 h. The t1DNA-QD 585 was purified by passing it through a filter tube of 100 kDa nominal molecular weight, and was blocked with 10% (v/v) blocking reagent for 0.5 h. Then, t1DNA-QD 585 was mixed with t2DNA at a ratio of 1 to 6. The hairpin DNA with a triple helix stem formed after shaking the mixture at 50 °C for 5 min and then cooling the mixture to room temperature. The TR-QD 585 was purified twice with centrifugation. The concentration of TR-QD 585 was determined by measuring the fluorescence intensity of QD 585 according to the working curve, $y = 79.415x + 335.35$ ($R^2 = 0.9964$). The asDNA-QD 655 was prepared following the previous procedure. The working curve of QD 655 was found to be $y = 93.434x + 286.3$ ($R^2 = 0.9953$).

ctDNA determination in PBS buffer

The TR-QD 585, the asDNA-QD 655, NaCl solution, the PBS buffer, and the model ctDNA in the PBS buffer were mixed. The mixture was defined as the reaction solution. The reaction solution was placed at 50 °C for 5 min and slowly cooled to room temperature. The reaction solution was left overnight at 4 °C in a refrigerator, the total concentration of QDs was

diluted to 0.05 nM before preparing the specimen. This diluted reaction solution was referred as the test solution. A portion (1.9 μL) of the test solution was dropped onto a positively charged glass slide, and immediately covered with a coverslip and sealed with nail polishing oil. The specimen was then ready for the single particle transmission grating-based spectral imaging. All the experiments were repeated at least three times. For each specimen, 10 domains were randomly imaged. For each domain, 50 frames were automatically taken placed in groups at a 300 ms intervals.

ctDNA determination in plasma

The amount of ctDNA in the plasma was determined following the previous procedure, except that the model ctDNA was replaced with a plasma sample or a plasma sample spiked with model ctDNA.

Single particle transmission grating-based spectral imaging

To take single particle image, the total concentration of QDs in the test solution was below 1.0 nM. An inverted Olympus IX71 fluorescent microscope with an EMCCD camera was used to take the transmission grating-based spectral images. The principle of transmission grating-based spectral microscope is illustrated in Scheme 1. A transmission grating was inserted between the optical outlet and the EMCCD camera, and divided a beam from an emitter into two beams. One beam in the shape of a dot was in the original propagation direction and referred to as the zeroth-order dot. Another beam in the shape of a streak was from the original propagation direction and referred as the first-order streak. The wavelength of the emitter complied with the equation, $\lambda = d1 \times d2/s$ ($d2$ is the distance between the grating and the EMCCD chip, s is the grating constant, $d1$ is the distance between the zeroth-order dot and the first-order streak). For a given microscope, λ was positively proportional to $d1$. Fig. 1A and B show the typical single particle spectral images of TR-QD 585 and asDNA-QD 655, respectively. The $d1$ of TR-QD 585 was obviously smaller than that of asDNA-QD 655. The $d1$ distribution of randomly selected QDs was plotted in Fig. 1C. The $d1$ distribution of TR-QD 585 did not overlap with that of asDNA-QD 655 at all.

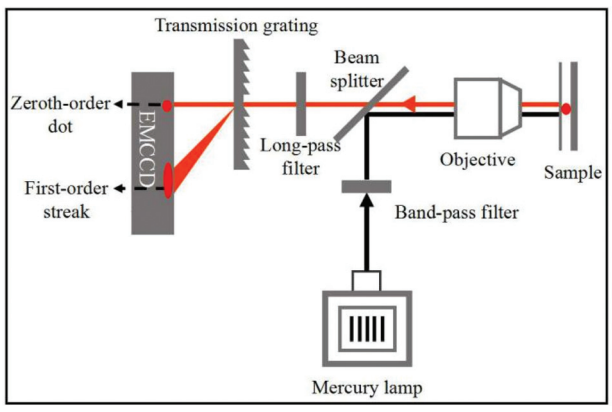

Scheme 1 The setup for single particle transmission grating-based spectral imaging.

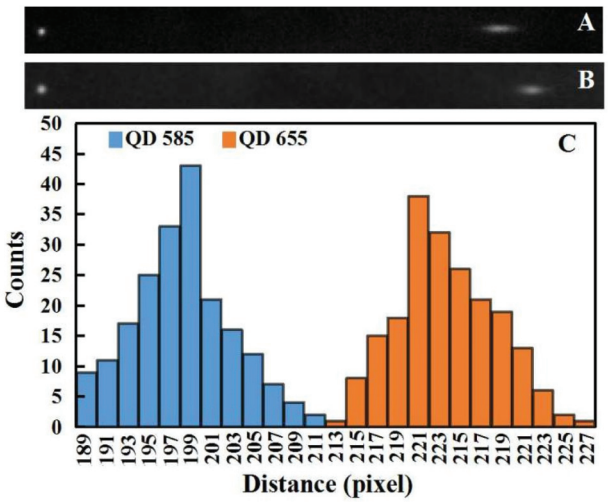

Fig. 1 Typical single particle spectral images of TR-QD 585 (A) and asDNA-QD 655 (B), and the distribution of the distance between the zeroth-order dot and the first-order streak (C).

Image analysis

Images were opened with ImageJ software. The zeroth-order dot and the first-order streak from the same fluorescent emitter were paired by position. The zeroth-order dots and the first-order streaks that could not be paired were excluded from the subsequent data analysis. The QDs and the QDs with two first-order streaks were counted. For each specimen, six domains were randomly selected and processed.

Results and discussion

Sensing mechanism

As shown in Scheme 2, the hairpin DNA containing a triple helix stem was immobilized onto a QD 585 (TR-QD 585). The hybridization between the target and the loop opened the stem. Consequently, asDNA immobilized onto a QD 655 (asDNA-QD 655) could hybridize with the opened DNA, yielding a two-color QD aggregate (QD 655 and QD 585). A two-color QD aggregate could be regarded as a target ctDNA. In theory, the maximum distance between the aggregated QDs was the sum of the lengths of the dsDNA a, dsDNA b, and dsDNA c (Scheme 2), and this was calculated to be 10.2 nm according to the distance of 0.34 nm between two neighboring base pairs. Because this distance was below the optical microscope resolution of 200 nm, the aggregated QDs could not be identified as individual objects but as one. When observed by transmission grating-based spectral microscopy, the distance between the zeroth-order dot and the first-order streak was in direct proportion to the emission wavelength. Therefore, it was deduced that: (1) the two-color QD aggregate showed a one zeroth-order dot because their dots overlapped, and (2) the two-color QD aggregate exhibited two first-order streaks

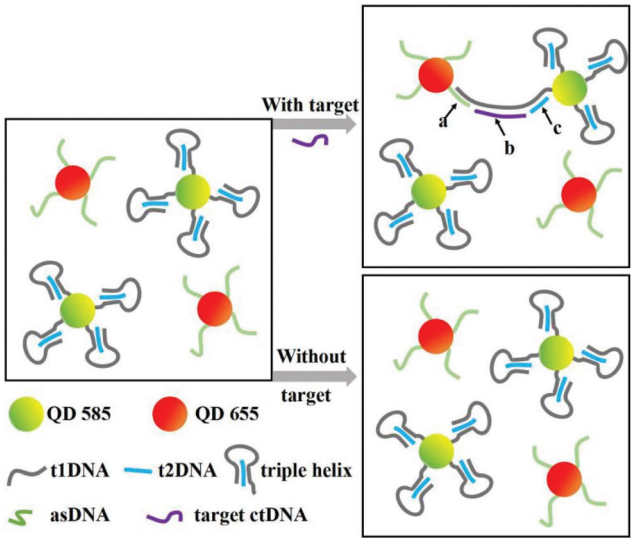

Scheme 2 The principle of the two-color QD aggregate formation.

because the streaks of TR-QD 585 and asDNA-QD 655 did not overlap. Conversely, the dispersed QDs presented one zeroth-order dot and one first-order streak. Therefore, the target ctDNA can be identified by the unique spectral pattern of the two-color QD aggregate: two first-order streaks.

The DNA sequence of the KARS gene which is related to lung cancer was used as the model ctDNA. The principle was tested by comparing the spectra of TR-QD 585 and asDNA-QD 655 in the presence of the target to that in the absence of the target. Typical spectral images are shown in Fig. 2A and B. The spectral patterns without the target were same, being one zeroth-order dot and one first-order streak. Conversely, when the target was present, the spectral patterns with one dot and two streaks appeared, which indicating that the target induced the two-color QD aggregates.

Optimization of the experimental conditions

The ratio of TR-QD 585 to asDNA-QD 655, NaCl concentration, and the total concentration of QDs in the reaction solution were optimized. The percentage of the two-color QD aggregates in the total QDs was used to weight the results, and is defined as the aggregate rate. Each value of the aggregate was determined from over 200 QDs. Fig. 3A–C show the relationship between the previously described parameters and the aggregate rate. The best results were obtained under the following conditions: a TR-QD 585 to asDNA-QD 655 ratio of 2 to 3, 300 mM NaCl, and 2.0 nM QDs in the reaction solution.

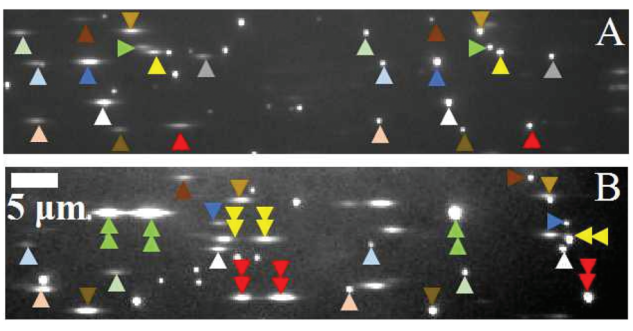

Fig. 2 Typical single particle spectral images of TR-QD 585 and asDNA-QD 655 with the target (A) and without the target (B). The zeroth-order dots and first-order streaks marked with triangles of the same color were paired.

The detection of ctDNA in PBS buffer

Under the optimized conditions, aggregate rates induced by the target at various concentrations were measured. Fig. 4 shows the relationship between the aggregation rate and the target concentration. The aggregation rate linearly increased with the target concentration in the range from 10.0 pM to

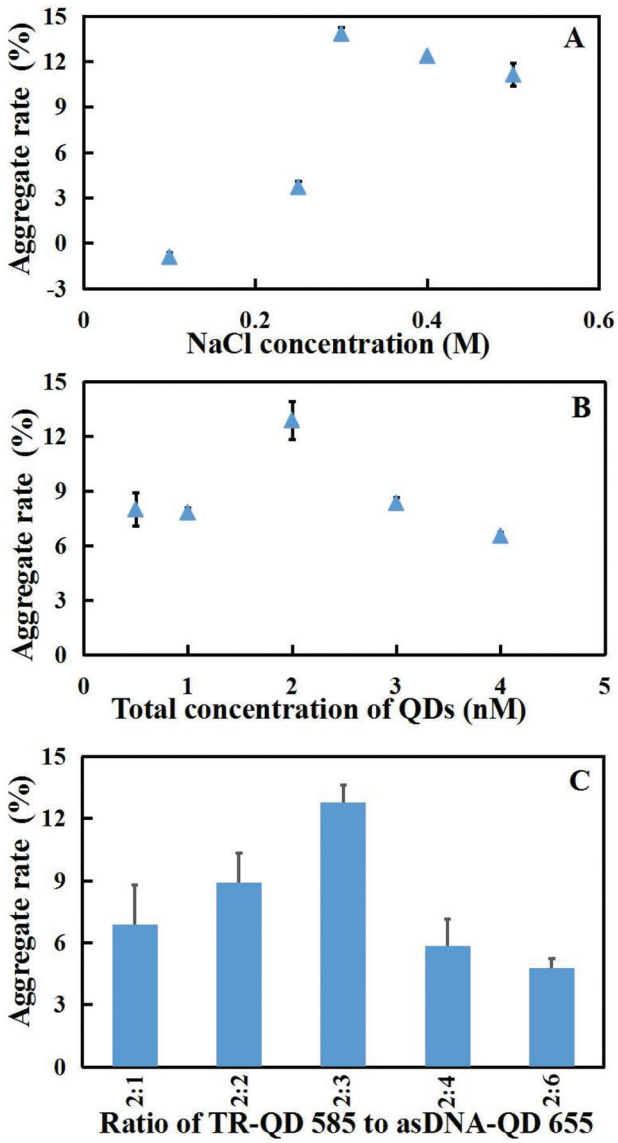

Fig. 3 Results of the optimization of the reaction solution: (A) NaCl concentration, (B) the total concentrations of the QDs, and (C) the ratio of TR-QD 585 to DNAr-QD 655.

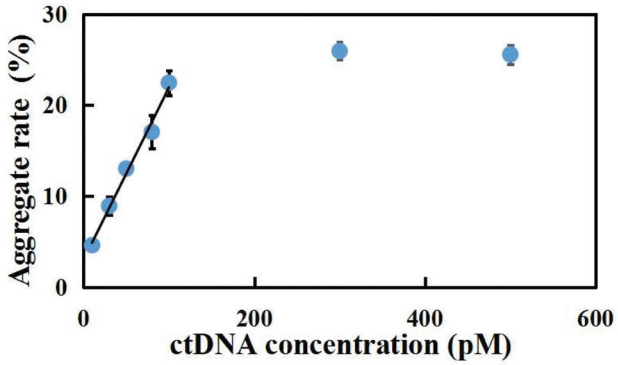

Fig. 4 The ctDNA working curve.

100.0 pM. The LOD was estimated to be 5.4 pM at a signal-to-noise ratio of 3σ, and the limit of quantification (LOQ) was calculated to be 34.5 pM at a signal-to-noise ratio of 10σ. A single judgement on the two-color QD aggregate was done within 2 min, which was an improvement when compared with that (more than 10 min) of the same-color QD aggregate.[23,24]

Reproducibility

Assay reproducibility was assessed by the response of the probes from different batches to the same sample. The aggregate rate of the four batches of probes remained constant as shown in Fig. 5, indicating the good reproducibility of the assay.

Selectivity and specificity

Good selectivity is required to accurately quantify ctDNA in a complex sample. To evaluate the selectivity, the aggregate rates induced by some species existing in blood were measured. The details are given in the caption of Fig. 6. The aggregate rates of these species were almost the same as that of the PBS buffer and far smaller than that of the target. This difference in the aggregate rates demonstrated that the probe had good selectivity. To further evaluate specificity, the effect of the DNA sequences on aggregate rate were investigated (Fig. 6). The aggregate rates of the non-matched DNA and the single-base mismatch DNA were close to that of the PBS buffer, and far

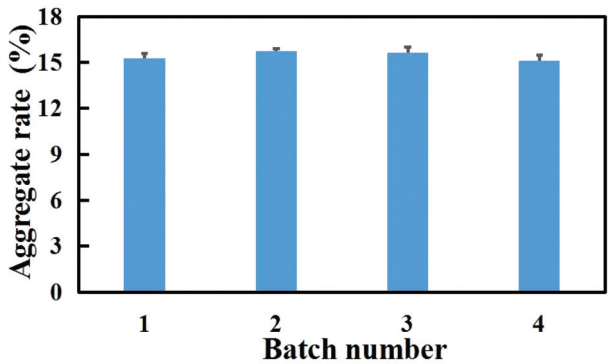

Fig. 5 Reproducibility data.

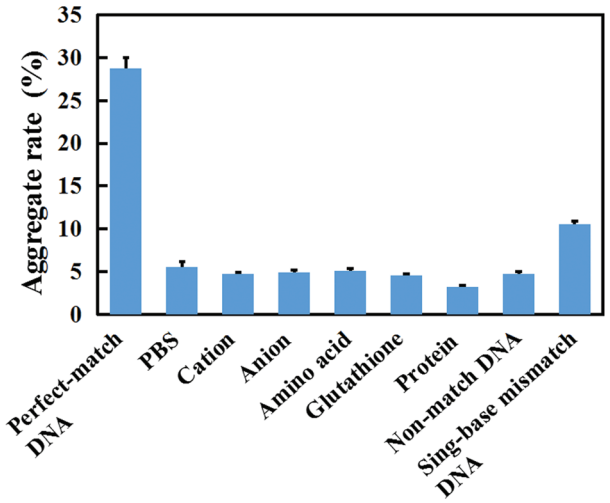

Fig. 6 Selectivity and specificity studies. Six cations, Mg^{2+}, Na^{+}, Cu^{2+}, Fe^{2+}, K^{+}, and Ca^{2+}; three anions, SO_4^{2-}, Cl^{-}, and CO_3^{2-}; 20 amino acids, proline, glycine, valine, glutamine, threonine, isoleucine, leucine, phenylalanine, tryptophan, alanine, methionine, tyrosine, histidine, cysteine, asparagine, aspartic acid, glutamic acid, lysine, arginine, and serine; and eight proteins, oval albumin, transferrin, human serum albumin, trypsin inhibitor, concanavalin A, lectin, epidermal growth factor, and fibrinogen, were tested for their selectivity and specificity. The concentration of each species was 10-fold higher than that of perfect-match DNA (ctDNA). Both the concentrations of non-match DNA and single-base mismatch DNA are the same as that of perfect-match DNA.

smaller than that of the perfect-match DNA. The discrimination factor (DF) is defined as:

$$\mathrm{DF} = \frac{\mathrm{AR_{pm}} - \mathrm{AR_{pbs}}}{\mathrm{AR_{ssm}} - \mathrm{AR_{pbs}}}$$

where $\mathrm{AR_{pm}}$, $\mathrm{AR_{pbs}}$, and $\mathrm{AR_{ssm}}$ represent the aggregate rates caused by the prefer-match DNA, the PBS buffer, and the single-base mismatch DNA, respectively. The DF was calculated to be 4.6. This value was better than the one given in a previously reported study,[25] implying that the probe had sufficient single-base discrimination capability.

Detection of ctDNA in plasma

To validate the practicability of directly quantifying ctDNA in blood, the recoveries of the plasma samples spiked with the target were measured. The spiked concentrations and the recoveries are summarized in Table 1. The recoveries ranged

Table 1 Plasma ctDNA recovery data

Sample	Added concentration (pM)	Found mean (pM)	Recovery (%)
1	30	27.6 ± 1.7	92 ± 5
	50	54.2 ± 1.5	108 ± 3
2	30	28.2 ± 1.4	94 ± 5
	50	49.6 ± 1.9	99 ± 4

from 92% to 108%, indicating the possibility of directly determining ctDNA in plasma.

Conclusions

The one-step quantification of ctDNA was achieved *via* identifying and counting target induced two-color QD aggregates. This approach showed the considerable ability to discriminate single-base mismatch DNA, and it has the potential for being used in the direct interrogation of ctDNA in plasma.

Conflicts of interest

There are no conflicts to declare.

Acknowledgements

Liu XJ is thankful for support from the Natural Science Foundation of China (NSFC 21775057).

Notes and references

1 M. Stroun, P. Anker, P. Maurice, J. Lyautey, C. Lederrey and M. Beljanski, Neoplastic characteristics of the DNA found in the plasma of cancer patients, *Oncology*, 1989, **46**, 318–322.
2 G. D. Sorenson, D. M. Pribish, F. H. Valone, V. A. Memoli, D. J. Bzik and S. L. Yao, Soluble normal and mutated DNA-sequences from single-copy genes in human blood, *Cancer Epidem. Biomar.*, 1994, **3**, 67–71.
3 S. Perakis, M. Auer, J. Belic and E. Heitzer, Advances in circulating tumor DNA analysis, *Adv. Clin. Chem.*, 2017, **80**, 73–153.
4 E. Yong, Written in blood DNA circulating in the bloodstream could guide cancer treatment - if researchers can work out how best to use it, *Nature*, 2014, **511**, 524–526.
5 D. A. Haber and V. E. Velculescu, Blood-based analyses of cancer: circulating tumor cells and circulating tumor DNA, *Cancer Discovery*, 2014, **4**, 650–661.
6 A. Campos-Carrillo, J. N. Weitzel, P. Sahoo, R. Rockne, J. V. Mokhnatkin, M. Murtaza, S. W. Gray, L. Goetz, A. Goel, N. Schork and T. P. Slavin, Circulating tumor DNA as an early cancer detection tool, *Pharmacol. Ther.*, 2020, **207**, 107458.
7 L. Cabel, C. Decraene, I. Bieche, J.-Y. Pierga, M. Bennamoun, D. Fuks, J.-M. Ferraz, M. Lefevre, S. Baulande, V. Bernard, S. Vacher, P. Mariani, C. Proudhon, F.-C. Bidard and C. Louvet, Limited sensitivity of circulating tumor DNA detection by droplet digital PCR in non-metastatic operable gastric cancer patients, *Cancers*, 2019, **11**, 396.
8 Z. Zou, P. Qi, Z. Qing, J. Zheng, S. Yang, W. Chen and R. Yang, Technologies for analysis of circulating tumour DNA: Progress and promise, *TrAC, Trends Anal. Chem.*, 2017, **97**, 36–49.
9 M. C. Maia, M. Salgia and S. K. Pal, Harnessing cell-free DNA: plasma circulating tumour DNA for liquid biopsy in genitourinary cancers, *Nat. Rev. Urol.*, 2020, **17**, 271–291.
10 M. Elazezy and S. A. Joosse, Techniques of using circulating tumor DNA as a liquid biopsy component in cancer management, *Comput. Struct. Biotechnol. J.*, 2018, **16**, 370–378.
11 S. L. Hayward, P. E. Lund, Q. Kang, A. Johnson-Buck, M. Tewari and N. G. Walter, Ultraspecific and amplification-free quantification of mutant DNA by single-molecule kinetic fingerprinting, *J. Am. Chem. Soc.*, 2018, **140**, 11755–11762.
12 J. Das, I. Ivanov, T. S. Safaei, E. H. Sargent and S. O. Kelley, Combinatorial probes for high-throughput electrochemical analysis of circulating nucleic acids in clinical samples, *Angew. Chem., Int. Ed.*, 2018, **57**, 3711–3716.
13 S. Campuzano, V. Serafin, M. Gamella, M. Pedrero, P. Yanez-Sedeno and J. M. Pingarron, Opportunities, challenges, and prospects in electrochemical biosensing of circulating tumor DNA and its specific features, *Sensors*, 2019, **19**, 3762.
14 F. Malentacchi, S. Pizzamiglio, P. Verderio, M. Pazzagli, C. Orlando, C. M. Ciniselli, K. Guenther and S. Gelmini, Influence of storage conditions and extraction methods on the quantity and quality of circulating cell-free DNA (ccfDNA): the SPIDIA-DNAplas external quality assessment experience, *Clin. Chem. Lab. Med.*, 2015, **53**, 1935–1942.
15 J. Das, I. Ivanov, L. Montermini, J. Rak, E. H. Sargent and S. O. Kelley, An electrochemical clamp assay for direct, rapid analysis of circulating nucleic acids in serum, *Nat. Chem.*, 2015, **7**, 569–575.
16 J. Das, I. Ivanov, E. H. Sargent and S. O. Kelley, DNA clutch probes for circulating tumor DNA analysis, *J. Am. Chem. Soc.*, 2016, **138**, 11009–11016.
17 J. Zhang, Y. Dong, W. Zhu, D. Xie, Y. Zhao, D. Yang and M. Li, Ultrasensitive detection of circulating tumor dna of lung cancer via an enzymatically amplified SERS-based frequency shift assay, *ACS Appl. Mater. Interfaces*, 2019, **11**, 18145–18152.
18 X. Lu, L. Wang, Q. Chen, Y. Wang, Z. Cao, G. Zhou and L. Li, A biosensor based on multifunctional allostery for dynamic analysis of circulating tumor DNA, *Chem. Commun.*, 2020, **56**, 4184–4187.
19 F. Ma, Y. Li, B. Tang and C.-Y. Zhang, Fluorescent biosensors based on single-molecule counting, *Acc. Chem. Res.*, 2016, **49**, 1722–1730.
20 J. J. Gooding and K. Gaus, Single-molecule sensors: challenges and opportunities for quantitative analysis, *Angew. Chem., Int. Ed.*, 2016, **55**, 11354–11366.
21 X. Liu, C. Huang, X. Dong, A. Liang, Y. Zhang, Q. Zhang, Q. Wang and H. Gai, Asynchrony of spectral blue-shifts of quantum dot based digital homogeneous immunoassay, *Chem. Commun.*, 2018, **54**, 13103–13106.

22 X. Shi, S. Dong, M. Li, X. Liu, Q. Zhang, W. Zhao, C. Zong, Y. Zhang and H. Gai, Counting quantum dot aggregates for the detection of biotinylated proteins, *Chem. Commun.*, 2015, **51**, 2353–2356.
23 S. Dong, X. Liu, Q. Zhang, W. Zhao, C. Zong, A. Liang and H. Gai, Sensing active heparin by counting aggregated quantum dots at single-particle level, *ACS Sens.*, 2017, **2**, 80–86.
24 X. Liu, Y. Sun, X. Lin, X. Pan, Z. Wu and H. Gai, Digital duplex homogeneous immunoassay by counting immunocomplex labelled with quantum dots, *Anal. Chem.*, 2021, **93**, 3089–3095.
25 X. He and N. Ma, A general strategy for label-free sensitive DNA detection based on quantum dot doping, *Anal. Chem.*, 2014, **86**, 3676–3681.